Development/Plasticity/Repair

Gap Junction Expression Is Required for Normal Chemical Synapse Formation

Krista L. Todd, William B. Kristan Jr, and Kathleen A. French
Division of Biology, Neurobiology Section, University of California, San Diego, La Jolla, California 92093

Electrical and chemical synapses provide two distinct modes of direct communication between neurons, and the embryonic development of the two is typically not simultaneous. Instead, in both vertebrates and invertebrates, gap junction-based electrical synapses arise before chemical synaptogenesis, and the early circuits composed of gap junction-based electrical synapses resemble those produced later by chemical synapses. This developmental sequence from electrical to chemical synapses has led to the hypothesis that, in developing neuronal circuits, electrical junctions are necessary forerunners of chemical synapses. Up to now, it has been difficult to test this hypothesis directly, but we can identify individual neurons in the leech nervous system from before the time when synapses are first forming, so we could test the hypothesis. Using RNA interference, we transiently reduced gap junction expression in individual identified neurons during the 2–4 d when chemical synapses normally form. We found that the expected chemical synapses failed to form on schedule, and they were still missing months later when the nervous system was fully mature. We conclude that the formation of gap junctions between leech neurons is a necessary step in the formation of chemical synaptic junctions, confirming the predicted relation between electrical synapses and chemical synaptogenesis.

Introduction

Neurons communicate with one another at electrical synapses, in which gap junction protein complexes allow ions and small biomolecules to pass between cells. Although electrical synapses were first characterized 50 years ago (Furshpan and Potter, 1959; Bennett et al., 1963), most synaptic research has focused on chemical synapses. There is, however, a growing appreciation that electrical synapses play important roles in mature neuronal circuits (Drapeau et al., 1995; Roerig and Feller, 2000), as well as in developmental processes such as neuronal differentiation (Bani-Yaghoub et al., 1999a,b), radial migration (Elias et al., 2007), and apoptosis (de Rivero Vaccari et al., 2007).

Electrical synapses may also shape the formation of chemical synapses in neuronal circuits. In many species [e.g., the optic lamina of *Daphnia* (Lopresti et al., 1974), rat cortex (Connors et al., 1983; Lo Turco and Kriegstein, 1991; Peinado et al., 1993), and ferret retina (Penn et al., 1994)], neurons form transient electrical synapses just before the appearance of chemical synapses. Similarly, axons regenerating in culture form electrical synapses before establishing appropriate chemical synapses (O'Lague et al., 1978; Szabo et al., 2004). In addition, observations in electrical synapse knockdown experiments have suggested a role in chemical synapse development. Connexin36 knock-out mice lack chemical synapses in their olfactory bulbs (Maher et al., 2009). In *Drosophila*, mutations in either of two gap junction genes produced impaired electrical and chemical synapses in the visual system, and transgenic expression of electrical synapses during development rescued chemical synaptic transmission in adults with these mutations (Curtin et al., 2002). Furthermore, studies of the neuromuscular junction revealed gross developmental dependence between electrical and chemical synapses (Chang et al., 1999; Personius et al., 2001, 2007). These correlations strongly suggest that transient electrical synapses are necessary in either the formation of chemical synapses (Fischbach, 1972; Szabo et al., 2004) or their activity-dependent refinement (Kandler and Katz, 1995), but the difficulty of modifying the development of individual identified neurons *in vivo* has been an obstacle to a direct and specific test of these hypotheses. However, in embryos of the medicinal leech, *Hirudo verbana* [previously grouped with *Hirudo medicinalis* (Siddall et al., 2007)], we can follow the development of many individually identified neurons from their initial neurite outgrowth to their incorporation into mature functional neural circuits (Stent et al., 1992). We used these robust and experimentally tractable embryos to ask whether gap junctions are necessary for chemical synaptogenesis. Even in embryos (Fig. 1*A*,*B*), the somata of the neurons in *H. verbana* ganglia are large (10–15 μm in diameter) (Marin-Burgin et al., 2005), they are in stereotyped positions (Dietzel and Gottmann, 1988; Marin-Burgin et al., 2005), and for chronic experiments, the ganglia are easily accessible through the body wall (Fig. 1*C*). In addition, the behavioral function of many leech neurons is known (Kristan et al., 2005), as is the developmental timeline of neuronal connectivity (Marin-Burgin et al., 2005) (Fig. 1*D*).

At least 12 different innexins (i.e., invertebrate gap-junction protein monomers) have been identified in *Hirudo* sp. (Dykes and Macagno, 2006), but *Hm*–inx1 is the only innexin that is expressed in all central neurons (Dykes et al., 2004). To test

Received May 6, 2010; revised Sept. 4, 2010; accepted Sept. 13, 2010.
This work was supported by National Institutes of Health Grants GM08107, MH43396, and NS35336 (W.B.K.). We thank Joyce Murphy for her skills in leech husbandry. We are grateful to Dr. Iain Dykes for useful conversations during the early stages of this project.
Correspondence should be addressed to Krista L. Todd, Division of Biology, Neurobiology Section, University of California, San Diego, 9500 Gilman Drive, La Jolla, CA 92093. E-mail: kltodd@ucsd.edu.
DOI:10.1523/JNEUROSCI.2331-10.2010
Copyright © 2010 the authors 0270-6474/10/3015277-09$15.00/0

whether gap-junction-based electrical connections are a necessary part of chemical synapse formation, we developed *in vivo*, single-cell RNA interference (RNAi) that transiently decreases the functional expression of *Hm*–inx1 early in synaptogenesis and observed the results of the manipulation at the molecular, cellular, synaptic, and behavioral levels.

Materials and Methods

Animals

Adult medicinal leeches (*Hirudo* sp.) were purchased from a commercial supplier (Leeches USA or Carolina Biological Supply) and maintained in a breeding colony in our laboratory. Embryos were released from their cocoons no earlier than 9 d after egg deposition and were then held at 20–24°C in "embryo water," that is, sterile-filtered Arrowhead spring water (Arrowhead Water) with 32 μmol of $MgCl_2$ and 40 μmol of $CaCl_2$ added per liter.

Staging

We determined the embryonic stage of each embryo using external morphological features that run from 0% (egg deposition) to 100% of embryonic development (ED) (Reynolds et al., 1998). Development proceeds at ~3% ED per day at 20°C. All experiments were performed in ganglia from the midbody of the animal (segments 7–15) to minimize the effects of the anteroposterior gradient of development in the leech; ganglia in this region differ by no more than 1% ED (Reynolds et al., 1998).

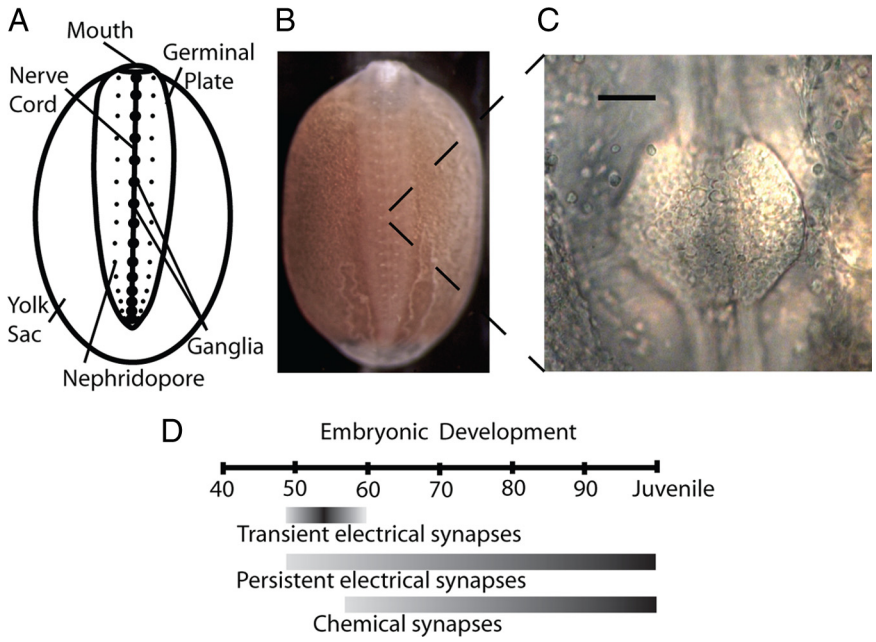

Figure 1. *Hirudo verbana* anatomy and timeline of synaptic development. ***A***, Anatomy of a leech embryo at ~50% of embryonic development (50% ED), the stage at which we injected dsRNA into neurons. The germinal plate develops on top of a yolk-filled sac; the embryo grows toward the posterior and expands left and right until it encircles the yolk sac. ***B***, Leech embryo at ~50% ED, the stage depicted in ***A***. The nerve cord is visible on the midline through the transparent body wall of the animal. This embryo is ~6 mm long. ***C***, The ventral surface of a segmental ganglion, viewed through a small incision in the body wall. Somata of ~200 neurons are visible in this ganglion. Scale bar, 50 μm. ***D***, Timeline for development of electrical and chemical synapses in *Hirudo* (modified from Marin-Burgin et al., 2005). Neurons lack processes before ~40% ED, and the leech becomes a juvenile at 100% ED. One day equals ~3% ED at room temperature (Reynolds et al., 1998).

Generating double-stranded RNA

We identified potential targets within the *Hm*–inx1 gene using an online algorithm provided by Ambion. Multiple, 21-base sequences were chosen and were individually generated by *in vitro* transcription with a Silencer siRNA Construction kit (Ambion). We usually injected a mix of two sequences targeting the *Hm*–inx1 mRNA (5′-AATAACTACAGCATGGAGAGG-3′ and 5′-AAGAGATCCGGAGTCAATATG-3′). A scrambled-control sequence (each nucleotide in the same abundance as in the first of the two sequences but arranged in a random order that is not homologous to any known gene) was also made (5′-AATCGAGAAGAGCTAAACTGG-3′). The concentrations of the resulting double-stranded RNAs (dsRNAs) were measured with a spectrophotometer, and the samples were held frozen at −20°C.

Neuronal injections

Adult. We dissected single midbody ganglia from adult leeches in normal leech saline (Muller et al., 1981) and pinned them in dishes coated with Sylgard (Dow Corning) to allow access to either the dorsal or the ventral neurons. Injections were performed on an Axioskop 2 (Carl Zeiss) equipped with both transmitted light and fluorescence optics. dsRNA fragments were diluted to 10–15 μM in 1.5% Alexa Fluor 488 dextran (10,000 molecular weight; Invitrogen) in sterile water and then wicked into sharp microelectrodes that had resistances of 60–80 MΩ if filled with 3 M potassium acetate (KAc). Target cells were identified and impaled under transmitted light. The dsRNA/Alexa Fluor mixture was pressure ejected (100 psi for 100–200 ms) using at ~1 Hz using a Picospritzer II (General Valve Corp.) and monitored using fluorescence optics. Because it was difficult to determine directly the volume injected into target neurons, we used an alternate criterion. Fluorescence images were obtained during the filling process using an AxioCam Hrc (Carl Zeiss) and AxioVision software (Carl Zeiss) set at standardized acquisition settings. As soon as the average somatic pixel intensity exceeded 80% maximum value, the injection was stopped. These ganglia were maintained in sterile L-15 culture medium until needed for assays. The same method was used for injections of scrambled control RNA and of Alexa Fluor 488 dextran vehicle controls.

Intact embryo, ventral neurons. We anesthetized embryos (50–60% ED) in diluted ethanol (8% EtOH in normal leech saline) and immobilized them ventral side up, held in place by two latex straps in a Sylgard trough. We visualized the nerve cord and ganglia with a dissection microscope and used a sharpened tungsten pin to make a small hole in the body wall above a target ganglion. Viewing through a compound microscope, we injected one of the solutions described above, using electrodes whose resistances were 80–100 MΩ when electrodes were filled with 3 M KAc. We then moved the injected embryos to a new 60 mm Petri dish containing 50% normal leech saline and 50% embryo water, where they healed and continued developing. After 2–3 hours, embryos were transferred into normal embryo water.

Determining number of dye-coupled neurons

We impaled, filled, and processed identified neurons as described previously (Marin-Burgin et al., 2005). Briefly, embryos were anesthetized, and targeted ganglia were exposed as described above. A combination of 2% (w/v) Neurobiotin (Vector Laboratories) and 2.5% (10,000 molecular weight) dextran Alexa Fluor 488 (Invitrogen) dissolved in deionized water was injected into cells using 500 ms pulses of 0.5–3 nA current. Filling was followed by visualizing the Alexa Fluor 488. The markers were allowed to diffuse for 1 h, and then we fixed the embryos in 2% paraformaldehyde in phosphate buffer, pH 7.4, for 2 h at room temperature. We then washed the embryos with PBS, permeabilized them with 0.3% Triton X-100 in PBS (PBX), and incubated them overnight in cyanine 3–streptavidin conjugate at 2 μg/ml in PBX (Jackson ImmunoResearch). The embryos were serially dehydrated in ethanol, cleared in methyl salicylate, and mounted in Gurr DePeX mounting medium (Electron Microscopy Sciences). We used standardized acquisition settings to obtain fluorescence confocal *Z*-stack images of the preparations (Bio-Rad), and the stacks were then processed using NIH ImageJ (http://rsbweb.nih.gov/ij/) to determine the average ± SD pixel intensity of the ganglion. We created a look-up table that displayed pixels with intensities

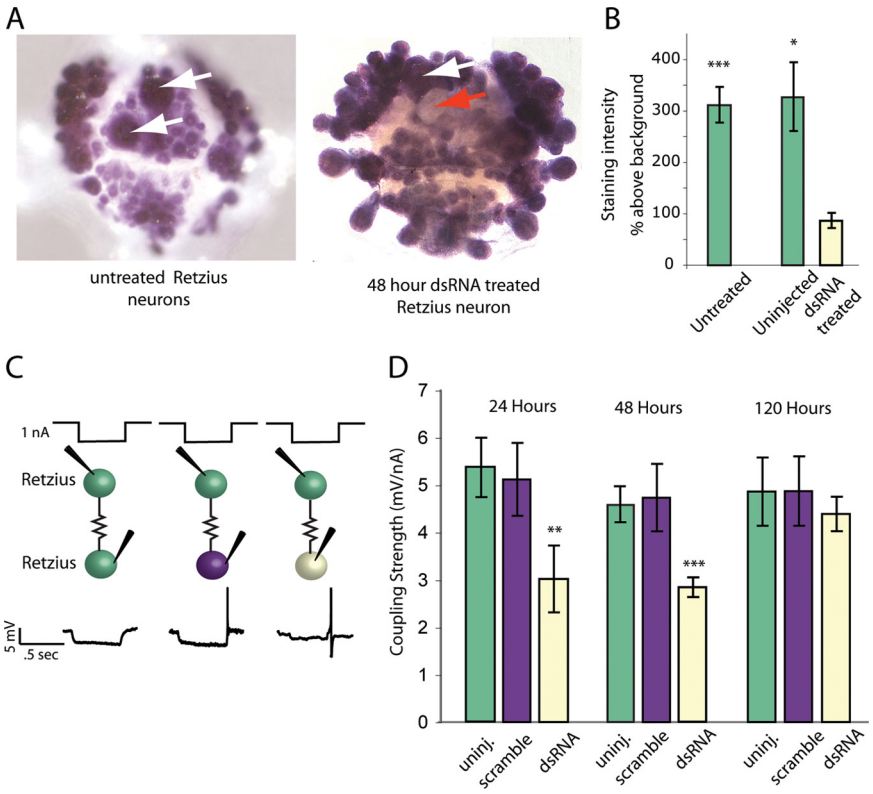

Figure 2. RNA interference decreased *Hm*–inx1 mRNA and coupling strength. ***A***, *In situ* hybridization using full-length *Hm*–inx1 probe and an adult leech ganglion produced dark staining (left) in all neurons, including untreated Retzius cells (white arrows), indicating high levels of *Hm*–inx1 mRNA in all neurons. mRNA levels decreased 48 h after dsRNA was injected into only one Retzius cell (red arrow), whereas the second, uninjected neuron stained darkly (white arrow). ***B***, Uninjected adult Retzius cells (in ganglia in which the second Retzius cell received an injection of dsRNA) and those in untreated ganglia stained more darkly than Retzius cells injected with *Hm*–inx1 dsRNA 48 h before staining ($n = 8$ untreated, 4 uninjected, and 4 RNAi treated; error bars show SEM; $*p < 0.05$, $***p < 0.001$). ***C***, Current and voltage traces of Retzius-to-Retzius electrical coupling. Half-second steps of hyperpolarizing current were passed into one Retzius cell (top of ***C***), and a voltage deflection was recorded in the other Retzius cell (bottom of ***C***). Green indicates an uninjected Retzius cell, purple a Retzius cell injected with scrambled dsRNA, and pale yellow a Retzius injected with dsRNA targeting *Hm*–inx1. Coupling strength was the slope of the line fitted to a plot of voltage change in the second cell as a function of the amount of current passed into the first cell. ***D***, Coupling strength in neurons was lower than normal at 24 and 48 h after dsRNA injection, and it returned to normal values by 120 h after the treatment. (24 h, $n = 10$ uninjected, 6 scramble injected, and 10 RNAi treated; 48 h, $n = 22$ uninjected, 12 scramble injected, and 20 RNAi treated; 120 h, $n = 7$ uninjected, 7 scramble injected, and 6 RNAi; Error bars show SEM; $**p < 0.01$, $***p < 0.001$). Color code is the same as in ***C***.

that exceeded 1 SD above the mean intensity and then examined each *Z*-stack, using the 1 SD threshold to identify coupled neurons.

In situ *hybridization*

To reveal Hm–inx1 mRNA, we used an *in situ* hybridization protocol as described by Dykes et al. (2004).

Electrophysiology

Adults. Adult ganglia were transferred from L-15 culture medium to cold, normal leech saline (Muller et al., 1981). We recorded on the stage of a compound microscope equipped with both transmitted light and fluorescence optics using sharp microelectrodes with resistances of 40–60 MΩ when filled with 3 M KAc. Intracellular signals were recorded with an Axoclamp-2A amplifier (Molecular Devices) operating in current-clamp mode. We stimulated and acquired data with a personal computer-based system using pClamp 9.0 software (Molecular Devices).

Embryos. We obtained electrophysiological recordings from embryonic neurons in a similar manner; only the differences will be noted. Under a dissection microscope, we placed the embryo on a Sylgard-coated glass slide, opened the body wall with a dorsal incision, and loosely pinned the body wall open to expose the dorsal surface of the ventral nerve cord. The embryo was moved to the compound scope and observed under fluorescence optics, which revealed Alexa Fluor 488 in the neuron that had been treated. The body anterior and posterior to the region around the target ganglion was removed, leaving six segments intact in the middle. Incisions were made over the target ganglion and over a control ganglion two segments away. Using a sharpened tungsten pin, the blood sinus was removed over each of these ganglia, and the body wall was pinned tightly all around. To further prevent motion artifacts, incisions were made at regular intervals in the body wall to sever longitudinal and oblique muscles. We recorded from neuronal somata using sharp microelectrodes that had resistances of 50–80 MΩ when filled with 3 M KAc. Embryonic neurons were extremely sensitive to osmotic changes, so we filled our electrodes with a solution of 120 mM potassium gluconate, which is nearly iso-osmotic with the external medium; their resistance was 200–600 MΩ. To prevent phototoxic damage, cells were illuminated very briefly during recordings.

Chemical EPSP amplitude. We measured the EPSP amplitude for chemical synapses by passing a current pulse into the presynaptic neuron (P cell) while recording from the postsynaptic neuron (AP cell). Because the AP neuron fires tonically at its resting membrane potential, EPSPs were more easily measured by silencing the AP with a 0.5 nA hyperpolarizing current injection. This current brought the membrane potential to −60 to −70 mV. EPSP amplitude in the AP neuron depends on its resting membrane potential attributable to an inward rectifying K^+ current (Wessel et al., 1999), but over this range the difference between EPSPs at rest and at −70 mV is <0.5 mV.

Electrical coupling strength. We measured the strength of an electrical synapse by passing multiple different current steps into one cell and recording the voltage responses in the coupled cell. These current steps were passed alternately into both cells of the pair. To compute the coupling strength, we divided the voltage response in the coupled cell by the stimulus current, using a custom program written in MATLAB; the slope of this line varies with the strength of coupling between the two cells. This quantity is often called the "transfer" or "mutual resistance" (Bennett, 1966) but we prefer to use the more intuitive term "coupling strength," and we report our results in units of millivolts postsynaptic per nanoampere presynaptic rather than in megaohms.

Behavioral assay

Video recording. Local bend behavior was elicited and video recorded using previously described methods (Baca et al., 2005). Briefly, we recorded the image of isolated body-wall preparations through a Wild dissection microscope using a C-Mounted Hitachi KP-M1 monochrome CCD camera (Image Labs International). The images were captured at 10 Hz for 15 s using a Data Translation frame grabber card (DT3155) controlled with the MATLAB (MathWorks) Image Acquisition Toolbox on a personal computer. On a separate computer, pulses from Axograph 4.9 software (Molecular Devices) synchronized video acquisition with the stimulus controller.

Body-wall stimulus. The leech was opened using a longitudinal ventrolateral incision made on the side opposite the pressure-sensitive mechanosensory neuron (P cell) of interest; P cells project ipsilaterally (Nicholls and Baylor, 1968). Most of the body was discarded, except for five segments centered on the target ganglion. We then denervated the two anterior and two posterior segments. To avoid stimulating the nociceptive sensory receptors in the segment being recorded, we pinned the body wall only in the denervated anterior and posterior ends. In these

preparations, we stimulated the receptive fields of either a Pd (P cell with a dorsal receptive field) or the ipsilateral Pv (P cell with a ventral receptive field) using five different stimulus force strengths, repeated three times in random order, with 3 min between trials to avoid habituation or sensitization. The force applied was quantified using a lab balance (Sartorius 1212 MP) placed under the preparation.

Contraction analysis. As described previously (Baca et al., 2005), we tracked the body-wall motion by computing optic flow estimates between successive image frames. We used the frame with the largest contraction during the local bend behavior to determine the maximal body-wall excursion within the targeted receptive field. Longitudinal body-wall motion within the three annuli anterior to the stimulus and at locations distributed circumferentially around the entire segment was then computed. (Each body segment consists of five rings called annuli.) This procedure yields a body-wall bend profile that displays the time integral of contraction distributed continuously around the body wall. We used these data to calculate the maximum and mean contraction within each quadrant of the leech.

Statistical analysis

ANOVA and *t* tests were used to evaluate statistical significance. Bonferroni's adjustments were made for multiple comparisons using InStat software. All error bars show the SEM.

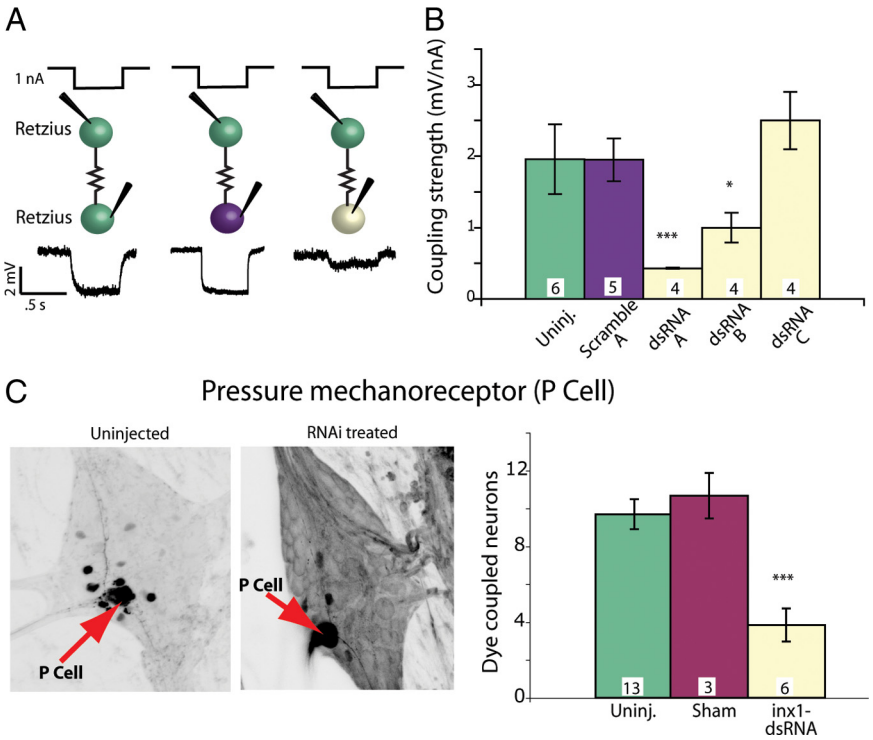

Figure 3. dsRNA targeting *Hm*–inx1 decreased function in embryonic electrical synapses. ***A***, Current and voltage traces of embryonic Retzius-to-Retzius electrical coupling. One nanoampere of hyperpolarizing current was passed into one Retzius cell for 0.5 s, and a voltage deflection was recorded in the other Retzius cell. Green indicates an uninjected Retzius cell, purple a Retzius cell injected with scrambled dsRNA, and pale yellow a Retzius injected with active dsRNA. Injections were made at 60% ED, and the recordings were performed 48 h later, at 66% ED. ***B***, Different dsRNA sequences produced different effects on electrical coupling. Sequences arbitrarily called dsRNAi A and dsRNAi B significantly decreased electrical coupling strength 48 h after treatment (numbers within each bar in ***B*** and ***C*** indicate the number of preparations of each type; ANOVA, $*p < 0.05$, $***p < 0.001$; significance is compared with both uninjected and scramble-injected preparations). ***C***, In each ganglion, a single mechanosensory P cell (red arrows) was injected with Neurobiotin; dark cells are neurons dye coupled to the Neurobiotin-injected P cell. The left image shows an untreated P cell; the right image shows cells dye coupled to the P cell 48 h after it was treated with inx1– dsRNA. The number of cells dye coupled to the P cell was significantly lower than control values for inx1– dsRNA-treated cells assayed 48 h after treatment (ANOVA, $p < 0.001$).

Results

Injecting dsRNA into a single adult neuron decreased the level of mRNA coding for *Hm*–inx1

To test whether RNAi could decrease cellular levels of innexin-1 mRNA, we used dsRNA that was 21 bp long and synthesized from chosen sequences within the *Hm*–inx1 gene. We used adult leeches and injected these dsRNAs into one of the pair of Retzius (Rz) neurons found in each midbody ganglion along the ventral nerve. After injection, the isolated ganglia were held in organ culture for several days. Normally, the two Rz cells within a ganglion are very strongly electrically coupled to each other (Hagiwara and Morita, 1962), and this electrical connection is echoed by the results of *in situ* hybridization using an *Hm*–inx1 probe in control ganglia (Fig. 2*A*). In contrast, 2 d after dsRNA was injected into one of a pair of Rz cells, the staining intensity of the treated Rz cell was <25% of the intensity in its untreated partner (Fig. 2*A*,*B*).

dsRNA treatment disrupted electrical synapse function

After injecting one of the paired Rz cells with dsRNA or a scrambled RNA and holding the ganglion in organ culture for 1–5 d, we used sharp microelectrodes to simultaneously impale both Rz cells in the ganglion. We applied a series of hyperpolarizing current steps to each neuron while recording the voltage deflection in the other (Fig. 2*C*). In untreated ganglia and in ganglia into which we injected a scrambled RNA, we recorded in the follower cell an average response of 5.4 ± 0.6 mV/nA (untreated) and 5.2 ± 0.8 mV/nA (scrambled) of current injected into the driven cell, regardless of which cell of the pair was driven. The electrical synapse between Rz cells is nonrectifying (Hagiwara and Morita, 1962), i.e., current flows between the cells equally well in either direction. After dsRNA treatment, this signal decreased significantly, to 3.0 ± 0.8 mV/nA at 24 h and 2.9 ± 0.2 mV/nA at 48 h after the treatment (Fig. 2*C*), regardless of which Rz cell was driven, and the coupling returned to normal values by 120 h after treatment. In addition, the input resistance measured in dsRNA-treated Rz cells was significantly higher than in controls, which is consistent with the loss of conductance channels in the membrane (11.2 ± 0.5 and 12.4 ± 0.7 MΩ in uninjected and scramble injected controls, 17.1 ± 1.5 MΩ in treated cells, $p < 0.4$)

Injecting the same constructs into Rz cells in embryos at 60% ED reduced the electrical coupling between Rz cells by >80% in 48 h compared with untreated neurons in the same embryos (Fig. 3*A*,*B*). We tested the efficacy of several dsRNA sequences targeting different portions of the *Hm*–inx1 mRNA and discovered that, as expected, not all dsRNAs performed equally well. Two sequences, dsRNA A (targeting the 5′ region) and dsRNA B (targeting the middle region) both yielded a significant decrease in coupling strength compared with uninjected and scrambled dsRNA-injected controls. dsRNA C had no effect. In the rest of our experiments, we combined dsRNA A and B in all injections, which we will call inx1–dsRNA.

A second measure of electrical synapse function is how readily the gap junctions pass small molecules. To test the ganglion-wide effect of decreasing *Hm*–inx1 in P cells, we injected inx1-dsRNA

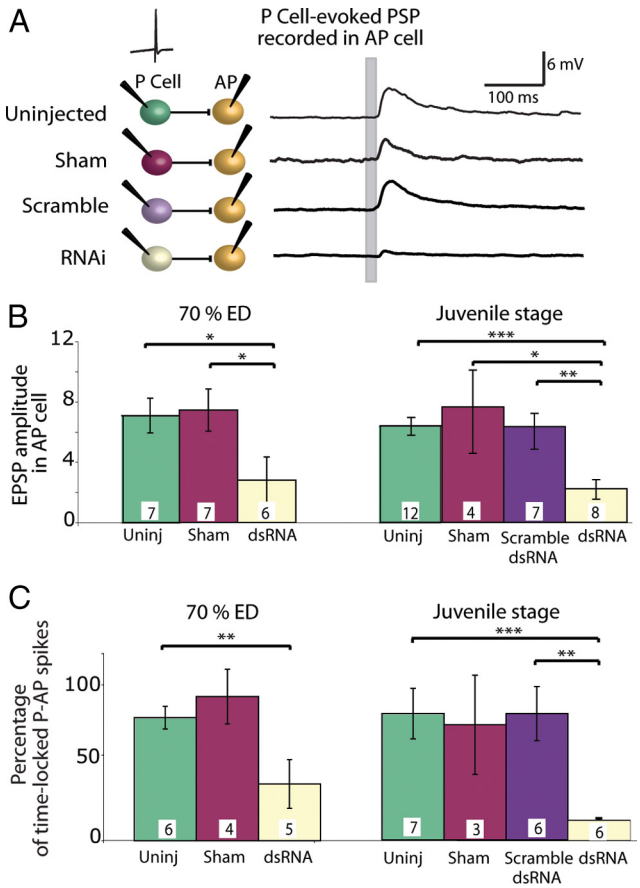

Figure 4. Blocking electrical synapses in embryos perturbed chemical synaptogenesis. ***A***, EPSPs in an AP cell in response to single spikes in a P cell within the same ganglion; the P cell spike occurred at the time marked by the gray bar on the AP recordings. AP cells were held hyperpolarized to silence their tonic firing. Each recording shown is from a single trial. Colors in the diagram are matched to the bars in ***B*** and ***C***. ***B***, EPSP amplitudes recorded in AP cells in response to P cell action potentials. When a P cell was treated with dsRNA before the onset of chemical synaptogenesis, it produced much smaller EPSPs in AP cells both 1 week after treatment (70% ED) and 3–5 weeks after treatment (juvenile stage) (ANOVA, $*p < 0.05$, $**p < 0.01$, $***p < 0.001$). ***C***, Probability of AP cell spikes in response to a spike in a P cell. Untreated, sham-treated, and scrambled dsRNA-injected P cells elicited a time-locked action potential in the AP cell ~80% of the time. Treating the P cell with dsRNA greatly reduced the incidence of time-locked action potentials in AP cells both at 70% ED and in the juvenile stage (ANOVA, $**p < 0.01$, $***p < 0.001$). Numbers within each bar in ***B*** and ***C*** indicate the number of preparations of each type.

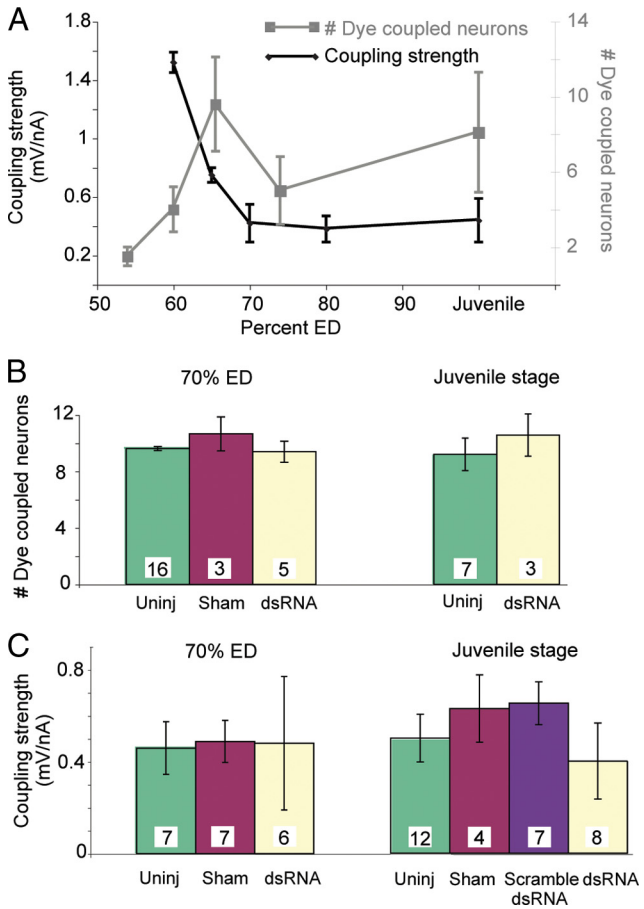

Figure 5. The electrical synapse between the P and AP cells returned to normal after RNAi. ***A***, Strength of the electrical synapse and dye coupling between the P cell and the AP cell in untreated ganglia. In black, the coupling strength between P and AP was strong early in development and waned but persisted at a lower level into adulthood. In gray, the number of neurons that were dye coupled to P cells increased to a steady state at the juvenile stage. ***B***, The number of neurons dye coupled to P cells injected with dsRNA returned to normal by 70% ED, i.e., 1 week after treatment, and persisted in juveniles. Green bars indicate the number of somata dye coupled to uninjected P cells, red to sham-injected P cells (injected with the vehicle Alexa Fluor 488), and pale yellow to P cells injected with inx1– dsRNA. ***C***, Electrical coupling strength between the P cell and the AP cell returned to the normal range 1 week after treatment and persisted into the juvenile stage. Green bars indicate the coupling strength from an uninjected P cell to the AP cell, red indicates sham-injected P cells (injected with the vehicle containing Alexa Fluor 488), purple indicates scrambled dsRNA-injected P cells, and pale yellow indicates P cells injected with inx1– dsRNA.

into one pressure-sensitive mechanosensory neuron (a P cell) in embryos at 65% ED, when electrical connections are well formed (Fig. 1*D*). We incubated the embryos for 48 h and then filled the treated cells with Neurobiotin (Vector Laboratories), a small molecule that passes through gap junctions between embryonic leech neurons (Fan et al., 2005; Marin-Burgin et al., 2006). After processing with fluorescently labeled streptavidin, we counted the number of neurons dye coupled to the treated neuron and found that the number was significantly reduced from control values (Fig. 3*C*). We concluded that intracellular injection of inx1–dsRNA reduced electrical synapses formed among leech neurons, as assayed by *in situ* hybridization, electrical coupling, and mobility of the small molecule Neurobiotin.

Weakening electrical synapses disrupted chemical synapse function

Previous work determined that *Hm*–inx1 mRNA is expressed in the nervous system beginning at ~48% ED (Dykes and Macagno, 2006), and electrical synapses can be detected electrophysiologically within 1 d, at ~51% ED (Marin-Burgin et al., 2005). In contrast, there is no indication of chemical synapses in embryonic ganglia until at least 2 d later, at ~55% ED (Marin-Burgin et al., 2005). To ask whether knocking down *Hm*–inx1 expression would affect chemical synaptogenesis, we used P cells because activating them elicits local bending (Thomson and Kristan, 2006), a leech behavior produced by a well characterized neuronal circuit (Kristan et al., 2005). Sensory input into the circuit comes primarily from the four mechanosensory P cells in each ganglion; each P cell is responsible for transducing pressure sensory information from a quadrant of the body wall within the segment in which the ganglion is located (Nicholls and Baylor, 1968; Lewis and Kristan, 1998c). When Neurobiotin is injected into an adult P cell, 12 other neurons within the same ganglion are labeled, and one of them is the contralateral AP cell, a motor-like neuron of unknown function. In adult *Hirudo* [as well as in

another leech species (Zhang et al., 1995)], the two neurons (P and AP) are connected by a robust monosynaptic excitatory chemical synapse made by the P cell onto the AP (Wessel et al., 1999), as well as by a weak electrical connection. We have found that, early in development, the coupling between these two neurons is completely electrical (data not shown).

We injected inx1–dsRNA into a single embryonic P cell at 48–50% ED, a time when innexin-based electrical synapses are initially forming and chemical synapses are not yet present (Fig. 1*D*) (Marin-Burgin et al., 2005). After the injection, we allowed the embryos to heal and to continue developing normally. One week later, at 70% ED, we simultaneously impaled P and AP cells with sharp microelectrodes to evaluate chemical synapses between the treated P cell and the contralateral AP cell (Fig. 4*A*) in the same ganglion. In control animals, the P cell had formed a strong chemical synapse onto the AP cell: action potentials in the P cell evoked robust EPSPs (7.1 ± 1.1 mV) in AP cells that had been hyperpolarized to silence tonic firing. In contrast, after inx1–dsRNA treatment of a P cell, action potentials in the P cell elicited in the AP cell EPSPs that were typically <1 mV (Fig. 4*A*,*B*). As a second measure of the strength of the P-to-AP synapse, we stimulated the P cell to produce single spikes and determined the percentage of trials in which these spikes elicited time-locked spikes in AP cells. In control (untreated, sham treated, and scramble dsRNA treated) ganglia, a spike in a P cell elicited a time-locked spike in the AP cell ~80% of the time, whereas after RNAi, P cell spikes elicited a significantly lower percentage of AP action potentials (45% lower) when compared with uninjected ganglia (Fig. 4*C*).

We knew from data presented in Figure 2*C* that injecting dsRNA had a transient effect that lasted no longer than 5 d in adult ganglia. To determine whether injecting dsRNA into neurons at 48% ED merely delayed the onset of chemical synaptogenesis, so chemical synapses would eventually develop after the electrical connections were reestablished, we injected dsRNA into P cells at 48% ED and then tested the strength of their synaptic connections onto AP cells when the leeches became juveniles, from 21 to 35 d after the injection. After this long period, the amplitude of EPSPs in AP cells remained small (Fig. 4*B*), and the percentage of P cell spikes that elicited a spike in the AP cell was low (Fig. 4*C*). We conclude that the severe weakening of the chemical synaptic connections produced by knocking down *Hm*–inx1 during electrical synaptogenesis was maintained long after embryogenesis was complete.

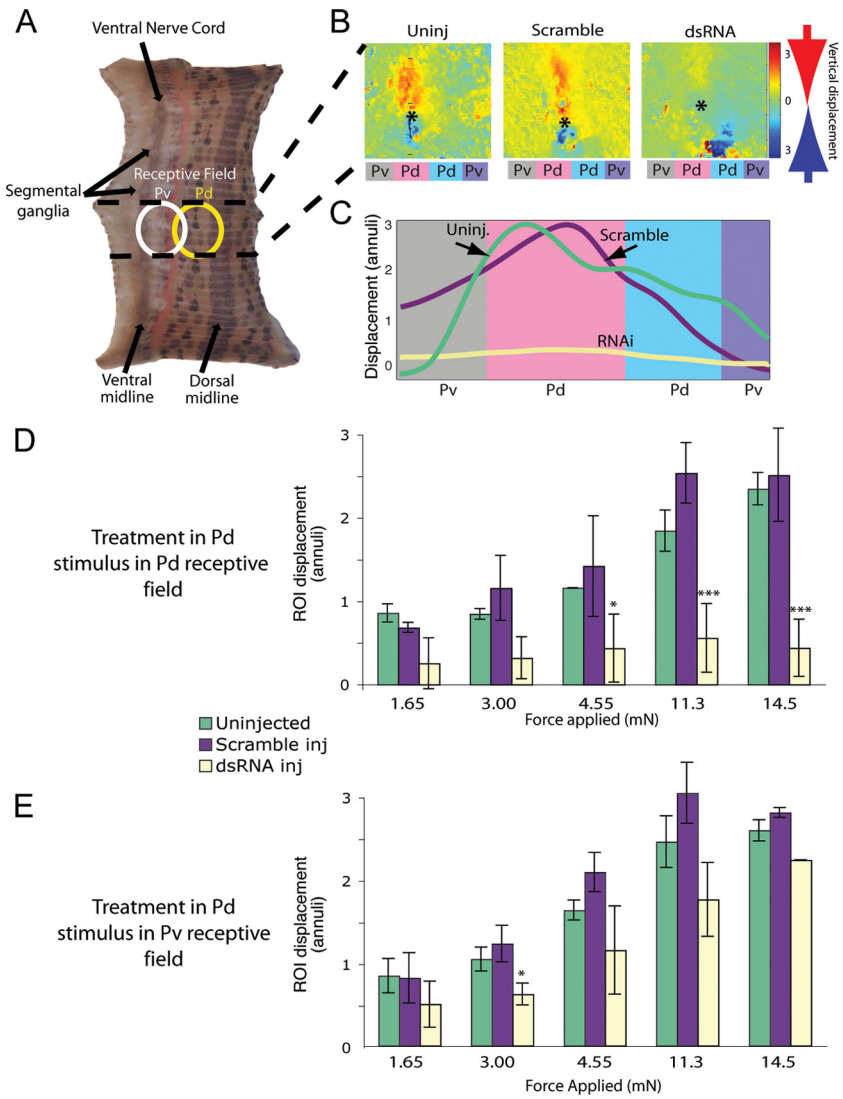

Figure 6. Stimulating dsRNA-treated P cells failed to elicit a behavioral response. ***A***, Seven-segment-long piece of body wall in which only the segment containing the treated P cell remained innervated (area between the dashed lines). We applied a tactile stimulus within the receptive field of the Pd (dorsal, yellow oval) or Pv (ventral, white oval). ***B***, Maximal longitudinal contraction after a stimulus in the receptive field of a Pd neuron. Using an optic flow algorithm (Baca et al., 2005), digital movies of contractions were converted to color-coded vector maps. Stimuli occurred at the asterisks; red indicates motion downward toward the point of touch, and blue indicates motion upward toward the touch. In both uninjected and scramble-injected controls, longitudinal movement is centered on the asterisk, indicating that the longitudinal contraction was focused on the stimulus. Colored rectangles below each image indicate the quadrant of the body wall innervated by each P cell: Pd indicates a dorsal quadrant, and Pv indicates a ventral quadrant on each side. ***C***, Longitudinal displacement in body-wall preparations after three different treatments: uninjected (green line), Pd injected with scrambled dsRNA (purple line), and Pd injected with inx1– dsRNA (pale yellow line). Amplitudes of movements within the region of interest (ROI), normalized to the anteroposterior dimension of an annulus, were integrated to yield a local bend profile (Baca et al., 2005). ***D***, Maximum displacement of the body-wall region of interest within the stimulated dorsal quadrant (contraction strength) as force increased (ANOVA with Bonferroni's *post hoc* analysis, $*p < 0.05$, $***p < 0.001$). ***E***, Ventral local bends in response to stimulating the receptive field of a Pv. Colors (which indicate how the ipsilateral Pd in the ganglion was treated) are the same as in ***D***; yellow bars show results of ventral stimulation in segments in which a Pd cell was injected with im1– dsRNA (ANOVA with Bonferroni's *post hoc* analysis, $*p < 0.05$, $***p < 0.001$).

We were concerned that the dsRNA-treated P cells might have induced a change in the input resistance of the postsynaptic AP cell. A significant change would have affected the inherent excitability of the AP cell producing the appearance of decreased synaptic strength. However, the input resistance of an AP cell in dsRNA-treated ganglia was not significantly different from controls when results were assayed in either 70% ED embryos or juvenile animals ($p = 0.34–0.7$ for 70% ED and $p = 0.2–0.4$ for juveniles). To address the excitability of the postsynaptic AP cells,

we compared the spontaneous firing rates of the AP cells in dsRNA-treated ganglia and control ganglia. The rates did not differ between the two types of cells ($p = 0.43$), so we conclude that the innate excitability of the postsynaptic AP cell is unaffected by treating a presynaptic P cell with dsRNA.

The diminished chemical synaptic strength could have been caused by a persistent decrease in the electrical connections. To test for this possibility, we first measured electrical connections in untreated animals. At the beginning of chemical synaptogenesis, P cells were electrically coupled to AP cells (Fig. 5*A*) through a connection with a coupling strength of ~1.5–2.5 mV/nA, which gradually waned over 1 or 2 d to a lower value (~0.5 mV/nA) that persisted into adulthood (Fig. 5*A*). During the same period, the number of cells that were dye coupled to the P cell increased. To determine whether electrical synapses were formed after the effects of inx1–dsRNA injection waned, we injected inx1–dsRNA into P cells at 48–50% ED and assayed for dye coupling and coupling strength at 70% ED and at juvenile stages (21–35 d after injection). At all stages tested, the number of cells dye coupled to inx1–dsRNA-treated P cells was not significantly different from controls (Fig. 5*B*). The location of leech neurons is somewhat variable so we could not determine with certainty whether every dye-coupled cell was identical with the cells that were dye coupled in control ganglia, but the patterns were very similar. In addition, the electrical coupling strength between treated P cells and AP cells was not significantly different from control values both at 70% ED and in juveniles (Fig. 5*C*). Thus, by these two measures, electrical coupling had returned to normal as the effect of the dsRNA waned, yet chemical synaptic connections remained significantly diminished (Fig. 4).

Effect of disrupted chemical synaptogenesis on normal behavior

Treating individual P cells with dsRNA reduced their chemical synaptic connections onto AP cells, but the role the AP cells play in generating or modulation leech behavior remains unknown. To assay the effect of this change in P cell synapses, we turned to the local bending response. Local bending is a segmental behavior (i.e., each segmental ganglion contains the full complement of identified neurons required to produce local bending in the home segment of the ganglion) that can be elicited by stimulating a single P cell (Lewis and Kristan, 1998b; Thomson and Kristan, 2006). Applying moderate pressure to the body wall stimulates one or two of the four P cells in a ganglion (depending on the location of the touch), which activates a single functional layer of interneurons that, in turn, activate appropriate motor neurons. In local bending, longitudinal muscles around the site of the touch contract while contralateral longitudinal muscles relax, bending the segment away from the touch. Local bending can be readily generated in a reduced (body wall) preparation consisting of a single ganglion connected to part or all of the body wall in that single segment. The piece of body wall can be used to stimulate the P cells mechanically and simultaneously to record the contractions of the muscles (Lockery and Kristan, 1991; Baca et al., 2005). In embryos at 50% ED, we injected inx1–dsRNA into a P cell (Pd) that innervates a dorsal quadrant of the body wall and then allowed the embryos to develop into juveniles. We made a body-wall preparation from the segment containing the treated Pd cell and applied mechanical stimuli of different intensities to the middle of its receptive field. As a control, we used an untreated P cell that innervated an adjacent, ventral quadrant (Pv) in the same segment (Fig. 6*A*). We used a digital video camera to record the body-wall movements made in response to the stimuli,

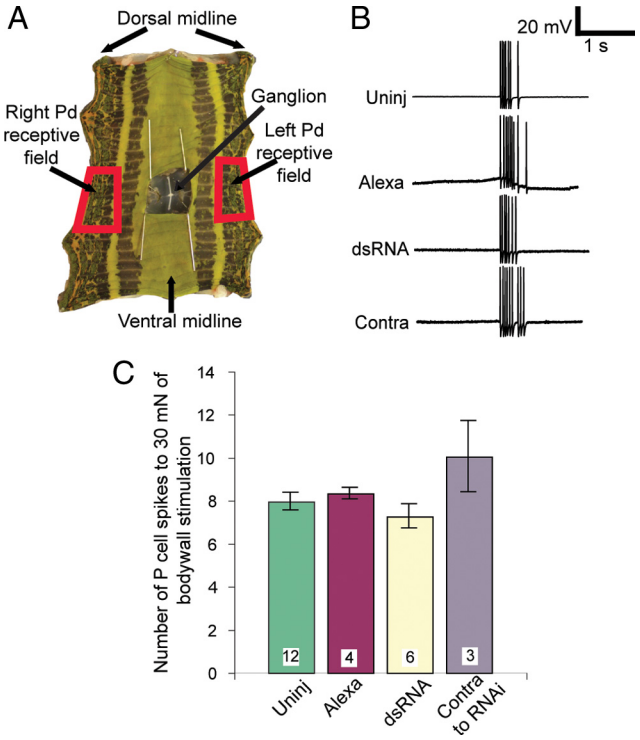

Figure 7. Treated P cells received and encoded sensory input normally. ***A***, The hole-in-the-wall preparation showing the one functionally innervated segment in a five-segment section of leech body wall. An incision was made along the dorsal midline, the piece of body wall was pinned flat, and the hole over the ganglion was enlarged and held open by pins. The receptive fields of the two Pd cells are indicated (red boxes). ***B***, Intracellular recordings from Pd cells in response to a brief (~500 ms) 30 mN stimulus in the receptive fields of the cell. "Contra" refers to the untreated Pd cell located on the side of the ganglion opposite to the inx1–dsRNA-treated Pd cell. ***C***, Number of spikes in a 500 ms time window after stimulation; the number of spikes elicited in an inx1–dsRNA-treated Pd cell was indistinguishable from controls. Color code as in Figures 4 and 5.

and then we used optic flow analysis to quantify longitudinal contractions (Zoccolan and Torre, 2002; Baca et al., 2005; Thomson and Kristan, 2006) (Fig. 6*B*,*C*). In control animals, we observed that stimuli in the receptive fields of either Pd or Pv caused the expected longitudinal contractions, and, as reported previously (Baca et al., 2005; Baca et al., 2008), stronger stimuli elicited stronger contractions (Fig. 6*D*,*E*). However, when we stimulated in the receptive field of the Pd cell that had been treated with inx1–dsRNA, we rarely observed local bending, and the contractions that did occur in this region were small and failed to increase with increasing stimulus intensities (Fig. 6*D*). In these animals, responses in the receptive field of the (untreated) Pv cell with a receptive field adjacent to the receptive field of the treated Pd cell elicited local bending that was indistinguishable from control animals (Fig. 6*E*).

There are two possible explanations for the lack of local bending response after inx1–dsRNA treatment: chemical synaptic transmission from the treated P cell onto local bend interneurons remained greatly reduced at this advanced development stage, or the sensory P cell was no longer effectively receiving and transducing stimulus information from the periphery. To test whether inx1–dsRNA-treated P cells reacted normally to sensory input, we used "hole-in-the-wall" preparations (Baca et al., 2008). Briefly, we produced the same kind of body-wall preparation shown in Figure 6*A*, except that we dissected away part of the body wall to expose the ganglion in the innervated segment (Fig.

7*A*). In these preparations, much of the ventral skin and all of the dorsal skin remains functionally innervated, and the number and frequency of spikes elicited in a P cell by mechanical force depends on the magnitude of the force, the location of the stimulus within the receptive field of the cell in the body wall, and the duration of the stimulus (Lewis and Kristan, 1998a). We recorded the number of spikes generated in Pd cells in response to brief, 30 mN pokes with a calibrated tungsten wire applied at the center of the receptive field of the cell (Fig. 7*B*). In addition to uninjected and sham-injected controls, this preparation provided an in-ganglion control: we recorded the response of the untreated contralateral Pd cell to the same stimulus applied in its own receptive field. Responses in Pd cells that were treated with dsRNA at 50% ED were indistinguishable from responses in uninjected, sham-injected, or contralateral P-cell controls (Fig. 7*C*). The experiments illustrated in Figures 6 and 7 show that the entire chemical synaptic output of the P cell (AP cells are not part of the local bending circuitry), but not its sensory input, was permanently reduced as a result of a brief, transient reduction in its electrical synapses during synaptogenesis.

Discussion

Our results indicate that electrical synapses must be established by a leech mechanosensory neuron while it is forming chemical synapses or it fails to make the chemical connections necessary for normal local bending behavior. Even weeks after the effect of RNAi had subsided and electrical coupling returned to normal, transmission through this behavioral circuit remained abnormal.

To reduce the expression of *Hm*–inx1 in early leech embryos, we used RNA interference, a technique that was invented in the 1990s for studying plants (Flavell, 1994) and fungi (Romano and Macino, 1992) and later refined for use in animal models (Fire et al., 1998). These early uses of RNA to block posttranslational gene expression were revolutionary in extending our understanding of the regulatory role of RNA within cells. The early application of this technology, however, required transforming or applying the knockdown to the whole organism. The refinement of molecular genetic techniques in recent years, using temperature-dependent expression of the RNAi phenotype and promoter-driven expression of active RNAi components, has greatly improved temporal and cellular specificity (Fortier and Belote, 2000; Brummelkamp et al., 2002; Napoli et al., 2009).

We have taken RNAi specificity a step farther by directly injecting dsRNA into a single, identified neuron that we can follow through development and into maturity. This method takes advantage of the well characterized behavioral circuitry and development of individual leech neurons and combines it with the targeted gene knockdown provided by RNA interference to transiently decrease the function of electrical synapses. It provides precise temporal control of gene expression at the single-cell level and allowed us to determine how expression of a single gap junction protein in a single cell at a particular phase during embryogenesis modified adult behavior.

Our finding that electrical synapses must be present in a neuron while it is forming chemical synapses or it fails to make those synapses confirms and strengthens a widely held hypothesis, but it in turn triggers questions regarding the mechanism: what are electrical synapses doing that allow chemical synapses to form between appropriate neurons? Perhaps gap junctions play an "active" role, e.g., transmission of some message or signal (either electrical or chemical) through the pore of the junction. Electrical synapses are notable for their ability to pass electrical activity rapidly and with high fidelity and for their conductance to ions and small molecules. Coordinated electrical activity has long been correlated with the formation and refinement of chemical synapses (Cohen-Cory, 2002). Even if direct current passage from one neuron to another through electrical synapses is not important, electrical synapses have been shown to modulate neuronal excitability within entire circuits (Rela and Szczupak, 2004). In addition to electrical activity, many ions and small molecules can pass through the pore formed at gap junctions. If electrical activity alone is not the synaptogenic factor, the role of gap junctions in directing or permitting chemical synaptogenesis might depend on passage of a chemical signal. Ions such as calcium and calcium-releasing second messengers such as IP_3 pass through gap junctions (Kumar and Gilula, 1996). These chemical species have been implicated as second messengers and synaptic transcriptional activators and could play a role in forming functional synapses.

Alternatively, there may be a physical—rather than a functional—explanation for the importance of electrical synapses. For instance, the adhesive quality of two hemichannels on apposing cells is required for neuronal migration after neural differentiation in mouse cortex (Elias et al., 2007). This observation suggests that electrical synapses might facilitate chemical synaptogenesis simply by holding two neurons in close enough proximity to allow other synaptogenic processes to proceed.

Distinguishing among the possible mechanisms will require additional experiments, but the unusually tractable nature of the developing leech nervous system, and the consequent ability to control expression of innexins one neuron at a time, will permit additional dissection of the relationship between gap junctions/electrical synapses and chemical synaptogenesis. We expect additional work to elucidate developmental mechanisms found in a wide variety of species.

References

Baca SM, Thomson EE, Kristan WB Jr (2005) Location and intensity discrimination in the leech local bend response quantified using optic flow and principal components analysis. J Neurophysiol 93:3560–3572.

Baca SM, Marin-Burgin A, Wagenaar DA, Kristan WB Jr (2008) Widespread inhibition proportional to excitation controls the gain of a leech behavioral circuit. Neuron 57:276–289.

Bani-Yaghoub M, Underhill TM, Naus CC (1999a) Gap junction blockage interferes with neuronal and astroglial differentiation of mouse P19 embryonal carcinoma cells. Dev Genet 24:69–81.

Bani-Yaghoub M, Bechberger JF, Underhill TM, Naus CC (1999b) The effects of gap junction blockage on neuronal differentiation of human NTera2/clone D1 cells. Exp Neurol 156:16–32.

Bennett MV (1966) Physiology of electrotonic junctions. Ann NY Acad Sci 137:509–539.

Bennett MV, Aljure E, Nakajima Y, Pappas GD (1963) Electrotonic junctions between teleost spinal neurons: electrophysiology and ultrastructure. Science 141:262–264.

Brummelkamp TR, Bernards R, Agami R (2002) A system for stable expression of short interfering RNAs in mammalian cells. Science 296:550–553.

Chang Q, Gonzalez M, Pinter MJ, Balice-Gordon RJ (1999) Gap junctional coupling and patterns of connexin expression among neonatal rat lumbar spinal motor neurons. J Neurosci 19:10813–10828.

Cohen-Cory S (2002) The developing synapse: construction and modulation of synaptic structures and circuits. Science 298:770–776.

Connors BW, Benardo LS, Prince DA (1983) Coupling between neurons of the developing rat neocortex. J Neurosci 3:773–782.

Curtin KD, Zhang Z, Wyman RJ (2002) Gap junction proteins expressed during development are required for adult neural function in the *Drosophila* optic lamina. J Neurosci 22:7088–7096.

de Rivero Vaccari JC, Corriveau RA, Belousov AB (2007) Gap junctions are required for NMDA receptor dependent cell death in developing neurons. J Neurophysiol 98:2878–2886.

Dietzel ID, Gottmann K (1988) Development of dopamine-containing neu-

rons and dopamine uptake in embryos of *Hirudo medicinalis*. Dev Biol 128:277–283.

Drapeau P, Catarsi S, Merz DC (1995) Signalling synapse formation between identified neurons. J Physiol Paris 89:115–123.

Dykes IM, Macagno ER (2006) Molecular characterization and embryonic expression of innexins in the leech *Hirudo medicinalis*. Dev Genes Evol 216:185–197.

Dykes IM, Freeman FM, Bacon JP, Davies JA (2004) Molecular basis of gap junctional communication in the CNS of the leech *Hirudo medicinalis*. J Neurosci 24:886–894.

Elias LA, Wang DD, Kriegstein AR (2007) Gap junction adhesion is necessary for radial migration in the neocortex. Nature 448:901–907.

Fan RJ, Marin-Burgin A, French KA, Otto Friesen W (2005) A dye mixture (Neurobiotin and Alexa 488) reveals extensive dye-coupling among neurons in leeches; physiology confirms the connections. J Comp Physiol 191:1157–1171.

Fire A, Xu S, Montgomery MK, Kostas SA, Driver SE, Mello CC (1998) Potent and specific genetic interference by double-stranded RNA in *Caenorhabditis elegans*. Nature 391:806–811.

Fischbach GD (1972) Synapse formation between dissociated nerve and muscle cells in low density cell cultures. Dev Biol 28:407–429.

Flavell RB (1994) Inactivation of gene expression in plants as a consequence of specific sequence duplication. Proc Natl Acad Sci U S A 91:3490–3496.

Fortier E, Belote JM (2000) Temperature-dependent gene silencing by an expressed inverted repeat in *Drosophila*. Genesis 26:240–244.

Furshpan EJ, Potter DD (1959) Transmission at the giant motor synapses of the crayfish. J Physiol 145:289–325.

Hagiwara S, Morita H (1962) Electrotonic transmission between two nerve cells in leech ganglion. J Neurophysiol 25:721–731.

Kandler K, Katz LC (1995) Neuronal coupling and uncoupling in the developing nervous system. Curr Opin Neurobiol 5:98–105.

Kristan WB Jr, Calabrese RL, Friesen WO (2005) Neuronal control of leech behavior. Prog Neurobiol 76:279–327.

Kumar NM, Gilula NB (1996) The gap junction communication channel. Cell 84:381–388.

Lewis JE, Kristan WB Jr (1998a) Representation of touch location by a population of leech sensory neurons. J Neurophysiol 80:2584–2592.

Lewis JE, Kristan WB Jr (1998b) A neuronal network for computing population vectors in the leech. Nature 391:76–79.

Lewis JE, Kristan WB Jr (1998c) Quantitative analysis of a directed behavior in the medicinal leech: implications for organizing motor output. J Neurosci 18:1571–1582.

Lockery SR, Kristan WB Jr (1991) Two forms of sensitization of the local bending reflex of the medicinal leech. J Comp Physiol A Neuroethol Sens Neural Behav Physiol 168:165–177.

Lopresti V, Macagno ER, Levinthal C (1974) Structure and development of neuronal connections in isogenic organisms: transient gap junctions between growing optic axons and lamina neuroblasts. Proc Natl Acad Sci U S A 71:1098–1102.

Lo Turco JJ, Kriegstein AR (1991) Clusters of coupled neuroblasts in embryonic neocortex. Science 252:563–566.

Maher BJ, McGinley MJ, Westbrook GL (2009) Experience-dependent maturation of the glomerular microcircuit. Proc Natl Acad Sci U S A 106:16865–16870.

Marin-Burgin A, Eisenhart FJ, Baca SM, Kristan WB Jr, French KA (2005) Sequential development of electrical and chemical synaptic connections generates a specific behavioral circuit in the leech. J Neurosci 25:2478–2489.

Marin-Burgin A, Eisenhart FJ, Kristan WB Jr, French KA (2006) Embryonic electrical connections appear to pre-figure a behavioral circuit in the leech CNS. J Comp Physiol A Neuroethol Sens Neural Behav Physiol 192:123–133.

Muller KJ, Nicholls JG, Stent GS (1981) Neurobiology of the leech. Cold Spring Harbor, NY: Cold Spring Harbor Laboratory.

Napoli S, Pastori C, Magistri M, Carbone GM, Catapano CV (2009) Promoter-specific transcriptional interference and c-myc gene silencing by siRNAs in human cells. EMBO J 28:1708–1719.

Nicholls JG, Baylor DA (1968) Specific modalities and receptive fields of sensory neurons in CNS of the leech. J Neurophysiol 31:740–756.

O'Lague PH, Furshpan EJ, Potter DD (1978) Studies on rat sympathetic neurons developing in cell culture. II. Synaptic mechanisms. Dev Biol 67:404–423.

Peinado A, Yuste R, Katz LC (1993) Gap junctional communication and the development of local circuits in neocortex. Cereb Cortex 3:488–498.

Penn AA, Wong RO, Shatz CJ (1994) Neuronal coupling in the developing mammalian retina. J Neurosci 14:3805–3815.

Personius K, Chang Q, Bittman K, Panzer J, Balice-Gordon R (2001) Gap junctional communication among motor and other neurons shapes patterns of neural activity and synaptic connectivity during development. Cell Commun Adhes 8:329–333.

Personius KE, Chang Q, Mentis GZ, O'Donovan MJ, Balice-Gordon RJ (2007) Reduced gap junctional coupling leads to uncorrelated motor neuron firing and precocious neuromuscular synapse elimination. Proc Natl Acad Sci U S A 104:11808–11813.

Rela L, Szczupak L (2004) Gap junctions: their importance for the dynamics of neural circuits. Mol Neurobiol 30:341–357.

Reynolds SA, French KA, Baader A, Kristan WB Jr (1998) Staging of middle and late embryonic development in the medicinal leech, *Hirudo medicinalis*. J Comp Neurol 402:155–167.

Roerig B, Feller MB (2000) Neurotransmitters and gap junctions in developing neural circuits. Brain Res Rev 32:86–114.

Romano N, Macino G (1992) Quelling: transient inactivation of gene expression in *Neurospora crassa* by transformation with homologous sequences. Mol Microbiol 6:3343–3353.

Siddall ME, Trontelj P, Utevsky SY, Nkamany M, Macdonald KS (2007) Diverse molecular data demonstrate that commercially available medicinal leeches are not *Hirudo medicinalis*. Proc Biol Sci 274:1481–1487.

Szabo TM, Faber DS, Zoran MJ (2004) Transient electrical coupling delays the onset of chemical neurotransmission at developing synapses. J Neurosci 24:112–120.

Thomson EE, Kristan WB (2006) Encoding and decoding touch location in the leech CNS. J Neurosci 26:8009–8016.

Wessel R, Kristan WB Jr, Kleinfeld D (1999) Supralinear summation of synaptic inputs by an invertebrate neuron: dendritic gain is mediated by an "inward rectifier" K^+ current. J Neurosci 19:5875–5888.

Zhang RJ, Zou DJ, Zheng J (1995) Correlation of receptive field position of mechanosensory neurons and the strength of their connections to AP neurons in the CNS of the leech (*Whitmania pigra*). Invert Neurosci 1:249–254.

Zoccolan D, Torre V (2002) Using optical flow to characterize sensory-motor interactions in a segment of the medicinal leech. J Neurosci 22: 2283–2298.